Cement and Concrete Research 38 (2008) 1297–1301

Contents lists available at ScienceDirect

Cement and Concrete Research

journal homepage: http://ees.elsevier.com/CEMCON/default.asp

Rheological behaviour of cement and silica suspensions: Particle aggregation modelling

Alice Chougnet [a,*], Thierry Palermo [b], Annie Audibert [c], Michel Moan [d]

[a] Etudes et Production Schlumberger, 1 rue Henri Becquerel, 92140 Clamart, France
[b] Institut Français du pétrole, 1 et 4 avenue de Bois-Préau, Rueil-Malmaison, France
[c] Total, France
[d] Université de Bretagne Occidentale, Brest, France

ARTICLE INFO

Article history:
Received 25 July 2006
Accepted 4 July 2008

Keywords:
Rheology
Cement
Silica
Aggregate

ABSTRACT

Cement and silica suspension rheological behaviour is modelled by supposing that particle aggregation occurs. With two independent parameters, the variation of the shear viscosity as a function of the shear rate for cement or silica suspensions having different solid volume fractions can be predicted. The model is in good agreement with experimental data. Cement suspensions are initially very similar to unreactive silica suspensions. The values of adhesion forces obtained seem to show that the effective interaction areas are very small. It reflects the fact that in the dormant period the particles are contacting at points, which become progressively higher in surface as C–S–H precipitates at these contacts. The model used is consistent with the observed power law variation of static and dynamic yield stresses with solid volume fraction. The aggregates formed under shear seem to be very compact, which is presumably related to the large solid volume fractions of the studied suspensions.

© 2008 Published by Elsevier Ltd.

1. Introduction

When a cement powder is mixed with water, it immediately begins to react and hydroxide, calcium, silicate, and aluminate ions are released in the water. The pH rapidly reaches high values and some hydrates precipitate on the surface of cement grains. After these initial hydration reactions, the rate of hydration is very low and remains very low during a few hours, the so-called “dormant period”. During this period, the cement paste is a suspension of particles having a very high negative surface charge density in water rich in divalent counterions (Ca^{2+}). Globally attractive forces between the particles are observed, and a possible mechanism by which the particles develop this cohesion can be found in the literature [1,2]. The interactions between particles result from the competition of an entropic pressure, a repulsive force originating from the “gas” pressure of the counterions, and an attractive force due to the correlations of ions located around neighbouring particles.

The aggregation of cement pastes is generally put forward to explain their rheological behaviour [3]. Actually without additives, these suspensions are thixotropic fluids presenting an apparent yield stress and a shear-thinning behaviour: these characteristics can be interpreted by the existence of globally attractive forces between cement particles that are responsible for the aggregation of the particles, the yield stress being linked to the gelation of the suspension, and the shear-thinning behaviour being explained by the progressive crumbling under shear. At high shear rate and for concentrated cement pastes, some authors also observed a shear-thickening behaviour, which could be due to the increase in the aggregate size under shear [3,4].

Otherwise, numerous theoretical models were proposed to describe the aggregation of suspensions [5–13]. They relate the viscosity of the suspension to the size of the aggregates. This aggregate radius results from the competition between the hydrodynamic forces, which tend to break the aggregates, and the cohesion forces, at the origin of the aggregation; it can be derived according to a mean-field approximation. The validity of these models was tested with many systems, such as red blood cells in saline suspensions [6], polystyrene latex [12], PMMA spheres in silicone fluids [7] and gas hydrate suspensions [14].

We propose here to model experimental data obtained with cement suspensions. The tests were performed during the “dormant period”. However, to be sure that the observed behaviour is not disturbed by the chemical evolution of the cement pastes during a rheological measurement, we have also studied silica suspensions as model systems.

2. Materials and methods

2.1. Cement and silica suspensions

The cement powder used, a class G Portland cement according to the American Petroleum Institute standards, is provided by

* Corresponding author.
E-mail address: alice.chougnet@espci.org (A. Chougnet).

0008-8846/$ – see front matter © 2008 Published by Elsevier Ltd.
doi:10.1016/j.cemconres.2008.07.001

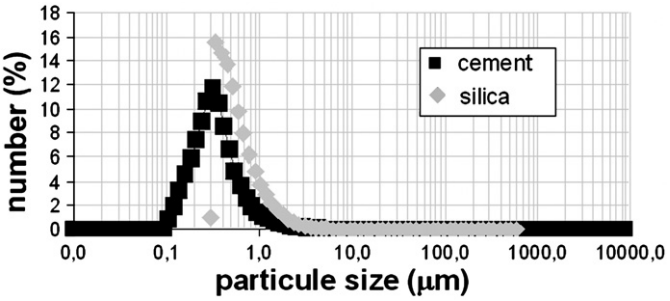

Fig. 1. Particle size distribution for cement and silica powders.

Dyckerhoff. It was studied by LASER granulometry with a Malvern Instruments apparatus: the powder particles are polydispersed in size, with an average number diameter of 0.6 μm (see Fig. 1). The cement suspensions are made by adding the powder to deionized water in a Waring blender, mixing at a speed of 4000 rpm during 3 min and 35 s at 1200 rpm.

Silica suspensions in lime saturated water are prepared in a Waring blender with a similar protocole as used for cement pastes. In order to have comparable systems, we have chosen SIFRACO C10 silica powder, which is constituted of ground quartz particles of the same sizes (with an average number diameter of 0.6 μm) as cement particles. According to Benhassaine and Bénézet [15,16], such a silica powder at 20 °C has a negligible pozzolanic reactivity compared to the time scale of a rheometrical experiment (a few hours); so unlike cement pastes, the model suspensions chosen do not chemically evolve because of hydration reactions.

Cement and silica suspensions having solid volume fractions comprised between 0.39 and 0.51 were studied. In Table 1, the mass ratios, *W*/*C* for cement suspensions and *W*/*S* for silica suspensions, are given as well as the solid volume fractions.

2.2. Rheological measurements

The rheological measurements were made using a stress controlled Haake RS150 rheometer, at 20 °C. To avoid slipping at the walls, a four blades vane geometry and a grooved stator were used [17]. The suspensions were first pre-sheared at 1000 s^{-1} for a few minutes and then allowed to rest until no more settling was observed (30 min for the cement suspensions and 40 min for the silica suspensions). The minimum settling height of all the tested suspensions, which was obtained for silica suspensions having a solid volume fraction of 0.39, was of 0.93 of the total height. So we neglected the modifications of the volume fraction due to settling. After those first two stages, in order to obtain flow curves, we performed increasing or decreasing shear stress steps. Each step lasted 60 s, which was a sufficient time to reach a steady flow.

3. Results and discussion

3.1. Rheological behaviour: increasing and decreasing stress steps

Fig. 2 represents the flow curves obtained for cement (a.) and silica (b.) suspensions, by applying increasing or decreasing shear stress steps; the observed behaviour is the same for both cement and silica

Table 1
Solid volume fractions and corresponding mass *W*/*C* (cement suspensions) and *W*/*S* (silica suspensions) ratios of the studied suspensions

Solid volume fraction ϕ	0.39	0.44	0.47	0.49	0.51
W/*C* (cement suspensions)	0.50	0.40	0.36	0.33	0.30
W/*S* (silica suspensions)	0.42	0.34	0.30	0.28	0.25

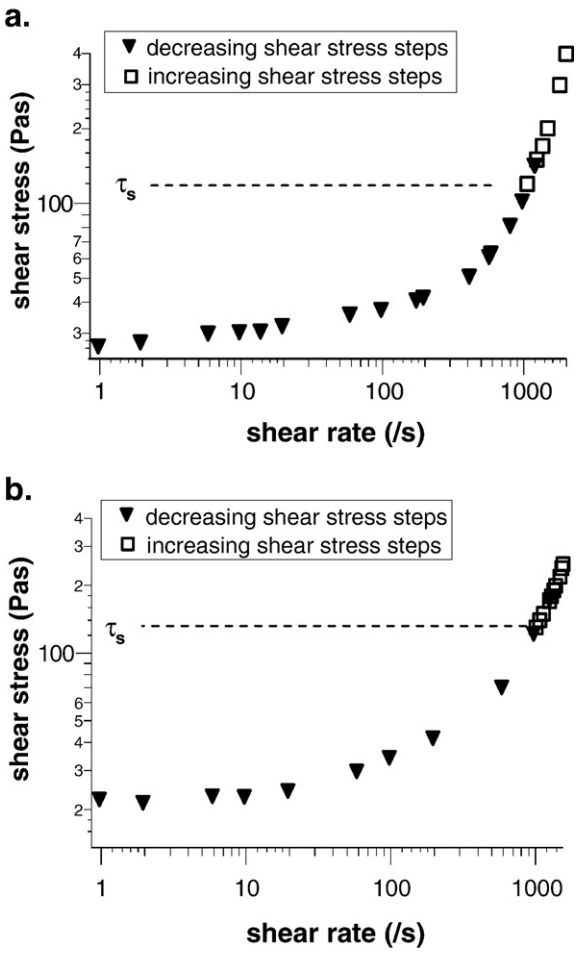

Fig. 2. Variations of the shear stress as a function of the shear rate for cement (a.) or silica (b.) suspensions of solid volume fraction 0.44. Increasing shear stress steps (□); decreasing shear stress steps (▼).

suspensions. So this behaviour cannot be attributed to the chemical evolution of the cement pastes, which are here studied before the acceleration of the hydration reactions. It can be seen that when the stress is increased, there is no flow until it reaches the apparent static yield stress τ_s, and then the shear rate rapidly reaches a very high value. The static yield stress reflects the gel state of the cement or silica. When the stress is decreased by steps from a value above τ_s, a shear-thinning behaviour, less drastic than what was obtained for increasing values of the stress, is observed. Data in steady state were obtained for shear rates between 2000 s^{-1} and 1 s^{-1}.

An apparent dynamic yield stress τ_s^{dyn} can be deduced by fitting these flow curves (decreasing stress steps) using for example the Casson [18] model. For each solid volume fraction, the dynamic yield stress τ_s^{dyn} is smaller than the static yield stress τ_s: the stress needed for the suspension to flow depends on its mechanical history. Whereas the static yield stress is obtained directly without extrapolation, the dynamic yield stress reflects a microstructure under dynamic condition of shear flow extrapolated from the lowest shear rate accessible (1 s^{-1} in this work). For example, for a cement suspension of a solid volume fraction of 0.44 (see Fig. 2), we obtain $\tau_s \approx 120$ Pa and $\tau_s^{dyn} \approx 25$ Pa. For a silica suspension having a solid volume fraction of 0.44, we obtain $\tau_s \approx 100$ Pa and $\tau_s^{dyn} \approx 20$ Pa.

The formation of aggregates in the suspension can explain the observation of an apparent yield stress, linked to the percolation of these aggregates which causes gelation, and of a shear-thinning behaviour, linked to the crumbling of these aggregates. More precisely, at each step, as a steady state is reached, the aggregate size reaches an

equilibrium size; and this means size increases when the applied stress is decreased. We now propose to describe quantitatively this last phenomenon.

3.2. Phenomenological model

We adopt here the same approach as proposed by Mills and co-authors in a series of papers [5–7] to describe the non-Newtonian behaviour of flocculated suspensions under shear flow conditions. This approach is mainly based on the following considerations: the size of aggregates under shear flow conditions is obtained with a mean-field approximation and an effective volume fraction is considered in lieu of the actual volume fraction. Similar microrheological models have also been developed by other authors over the last two decades [8–13].

Aggregates are characterized by a power law linking the number of particles per aggregate N with the particle radius a and the aggregate radius R:

$$N \propto \left(\frac{R}{a}\right)^{f}. \tag{1}$$

A prefix constant close to unity can be introduced in the right-hand term of the above expression depending on the definition of the characteristic length R, which can be the dynamic radius, the collision radius, the radius of gyration or the radius of circumscribed sphere [19]. In the following, as only proportional relationships will be used, this constant will be neglected.

Under shear conditions, at a given shear stress τ (or a given shear rate), the steady state is reached when the aggregates reach their mean equilibrium size R. The steady-state size can be predicted either from the balance between aggregate cohesion and flow related stresses or from competition between aggregation and fragmentation dynamics. Two modes of floc rupture are generally considered: surface erosion and large-scale fragmentation [20]. For floc fragmentation, cases of "rigid" flocs and "soft" flocs can be distinguished [21]. The papers on microrheological models [5–13] cited above also include discussions on floc size.

Experiments on low concentration systems or models dealing with isolated aggregates yield a scaling expression of the form [20]:

$$\frac{R}{a} \propto \left(\frac{F_a/a^2}{\eta_0 \dot{\gamma}}\right)^{m}. \tag{2}$$

where η_0 is the dynamic viscosity of the suspending fluid, $\dot{\gamma}$ the shear rate and m a constant; F_a, the adhesion force, is defined as the force to be applied to separate the particles at an infinite distance from each other. For finite volume fractions, in the mean-field approximation, the stresses withstood by the aggregates are the same as the ones generated by a continuum having the mechanical properties of the bulk suspension. Thus, the viscosity of the suspending fluid η_0 can be substituted by the viscosity of the suspension η [5,9,10]. We thus have:

$$\frac{R}{a} \propto \left(\frac{F_a/a^2}{\tau}\right)^{m} \tag{3}$$

with $\tau = \eta\dot{\gamma}$

Aggregates are supposed to behave like spheres composed of particles in contact which trap fluid. An effective volume fraction ϕ_{eff} is therefore introduced, related to the actual volume fraction ϕ by:

$$\phi_{\text{eff}} \propto \phi \left(\frac{R}{a}\right)^{(3-f)}. \tag{4}$$

The material law chosen is a viscosity function proposed by Mills [5–7]: the effective volume fraction ϕ_{eff} is introduced in his equation expressing the relative viscosity η_r as a function of the volume fraction and the maximum packing ability $\phi_{\max}$.

$$\eta_r = \frac{(1-\phi_{\text{eff}})}{\left(1-\frac{\phi_{\text{eff}}}{\phi_{\max}}\right)^{2}} \tag{5}$$

At the equilibrium, since the aggregate sizes are supposed to be closed to their mean value, we suppose that $\phi_{\max} = 4/7$, which is the maximum packing ability of randomly packed monodisperse spheres.

3.3. Determination of the microstructure parameters

By combining Eqs. (3) and (4), we get:

$$\frac{\phi_{\text{eff}}}{\phi} \propto \left(\frac{F_a}{a^2}\right)^{m(3-f)} * \left(\frac{1}{\tau}\right)^{m(3-f)}. \tag{6}$$

Moreover, by using Eq. (5), ϕ_{eff} can be determined from the experimental shear viscosities obtained for suspensions of different solid volume fractions ϕ and for shear rates between 1 s^{-1} and 2000 s^{-1}. The ratio ϕ_{eff}/ϕ is represented as a function of τ^{-1} in Fig. 3a for cement suspensions and in Fig. 3b for silica suspensions. In both cases, it can be noticed that ϕ_{eff}/ϕ varies as a power law of τ. Thus we can write, by introducing the parameters K and x:

$$\frac{\phi_{\text{eff}}}{\phi} = K\left(\frac{1}{\tau}\right)^{x}. \tag{7}$$

The x exponent corresponding to $m(3-f)$ is equal to 0.09 and to 0.07 for cement and silica suspensions, respectively. The obtained prefix constant K allows us to get an order of magnitude for $(F_a/a^2)^{m(3-f)}$. We obtain $K = 1.7$ $(\text{N/m}^2)^{m(3-f)}$ and $K = 1.6$ $(\text{N/m}^2)^{m(3-f)}$ for cement and silica suspensions, respectively. These values are very close, as are the flow curves obtained for the two suspensions.

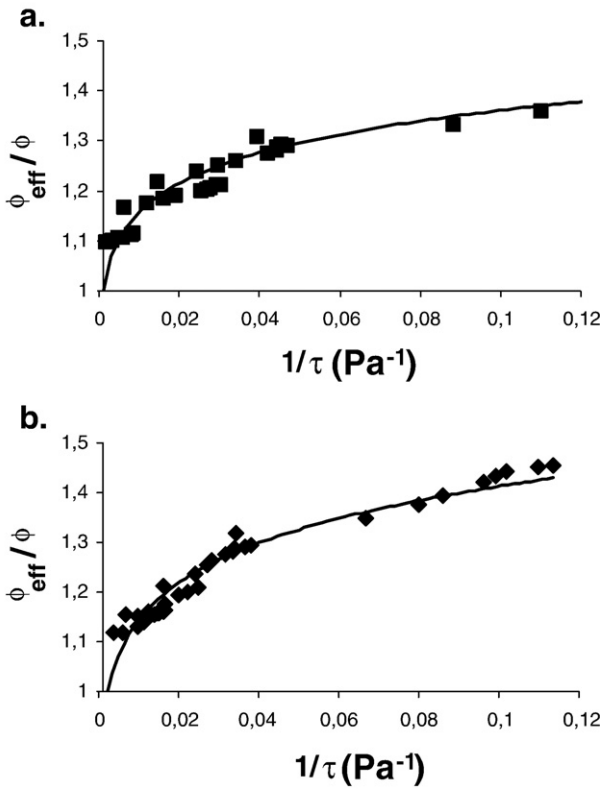

Fig. 3. Variations of the ϕ_{eff}/ϕ ratio as a function of the inverse of the shear stress τ for cement (a.) or silica (b.) suspensions. The full lines are power law fits.

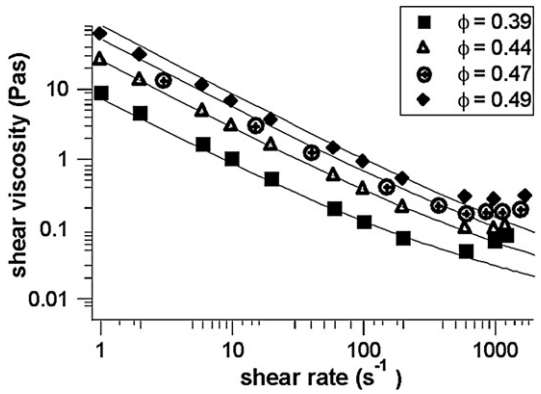

Fig. 4. Comparison between model (full lines) and experiment for cement suspensions.

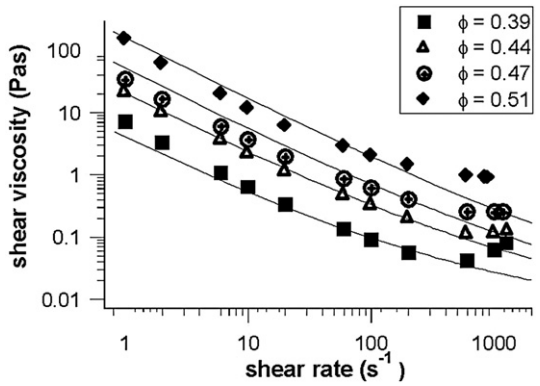

Fig. 5. Comparison between model (full lines) and experiment for silica suspensions.

The f exponent can then be determined, depending on the value of m, which is not precisely known. m depends on the mechanism of floc breakup and on the structure of aggregates. However, the values reported in the literature are usually in the range of 0.3 [21–23] to 0.7 [24]. This gives the f parameter for the two systems (cement and silica) in the range of 2.7 to 2.9. Such an order of magnitude is very high and indicates a high compactness of the particles in the aggregates. Typical values of f for perikinetic aggregation (caused by Brownian motion) vary between 1.8 and 2.1. However, it has been reported that values of f for orthokinetic aggregation (caused by medium flow) is generally much higher and may exceed 2.5 [22,23]. It can also be noticed that these high values of f do not mean that the aggregates have no porosity, since porosity also depends on the prefix constant we have neglected here.

As prefix constants were neglected in the above relationships, only an order of magnitude can be deduced for the force of adhesion F_a. With $a \approx 0.3$ μm, we have F_a in the range of 0.01–0.1 nN. This range of magnitude can be compared with the one obtained by Plassard et al. [25], who studied the forces of adhesion between the main hydration products of cement, which are the calcium silicate hydrates "C–S–H". Actually the nature of the cohesion forces is presumed to be partly the same in fresh cement suspensions as in set cement pastes [26], at the nano- and mesoscale [27]: it is the so-called correlation pressure caused by correlations between counterions on either side of the midplane of two charged particle surfaces [1,2].

Plassard et al. [25] measured the adhesion force between a micrometric flat C–S–H surface and a C–S–H nanocrystal at the top of an AFM tip immersed in a lime saturated solution. For similar conditions to ours (pH = 13 and $[Ca^{2+}] \approx 20$ mM), they found a force of about 1 nN. In this case, the measurements corresponded to interactions between two planes of C–S–H with an area of surface interaction estimated to $S_{int} = 64$ nm^2. The comparison between our results and the ones obtained by AFM allows us to estimate the effective area of surface interaction between particles in aggregates: $S_{int} \approx 0.6$–6 nm^2. This small value reflects the fact that the particles are initially contacting only at points, which become progressively higher in surface as C–S–H precipitates at these contacts when cement sets. Since only a small amount of C–S–H can be found between particles, the iono-covalent forces between individual C–S–H [27] can be neglected to calculate this area of surface interaction. This hypothesis seems consistent with the fact that very similar results were obtained in silica suspensions, in which the cohesion is only assured by physical forces.

3.4. Comparison between model and experiment

The respective values of $x = m(3-f)$ and $K \propto (F_a/a^2)^x$ being determined, the rheological behaviour of suspensions of any solid volume fraction can be deduced. And as can be seen in Fig. 4 for cement suspensions and Fig. 5 for silica suspensions, the predicted curves are fitting well experimental data, in the shear-thinning zone. In this zone, the best fit is obtained for the lowest solid volume fractions and the highest shear rates.

As the model used here supposes that there is a decrease of the aggregate size with shear rate, the data in the shear-thickening zone have not been taken into account for the determination of K and x. The shear-thickening behaviour which is observed here at high shear rates might be explained by the re-aggregation of particles [28]. It has already been observed in cement or silica pastes [3,4].

A minimum of viscosity η_{min}, i.e. the viscosity corresponding to the onset of the shear-thickening behaviour, can be defined. This value increases with the solid volume fraction, as can be seen in Figs. 4 and 5.

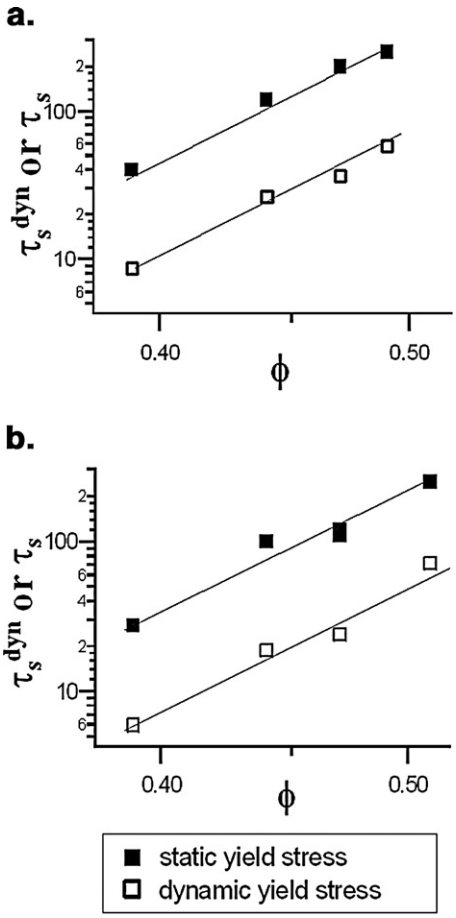

Fig. 6. Dynamic yield stress τ_s^{dyn} and static yield stress τ_s represented as functions of solid volume fraction for cement (a) or silica (b) suspensions.

It can be thought that as the minimum of viscosity is obtained at high shear rates, the aggregates are then completely broken. If it were the case, the effective volume fraction ϕ_{eff} would be equal to the solid volume fraction ϕ. But the values of ϕ_{eff}/ϕ are comprised between 1.3, for cement or silica suspensions of the smaller solid volume fraction, and 1.1 for those of higher solid volume fraction. Supposing that f is equal to 2.8, it means that aggregates of 4 to 40 particles remain even at the minimum of viscosity (which corresponds to aggregate radius between 0.5 and 1 μm).

3.5. On the yield stress

The dynamic yield stress τ_s^{dyn} can be expressed by extrapolating the value of the shear stress at the zero limit of shear rate, also corresponding to an effective volume fraction ϕ_{eff} that tends to ϕ_{max}. The substitution of ϕ_{eff} by ϕ_{max} and of τ by τ_s^{dyn} in Eq. (6) leads to:

$$\tau_s^{dyn} \propto \frac{F}{a^2}\left(\frac{\phi}{\phi_{max}}\right)^{\frac{1}{m(3-f)}}. \quad (8)$$

which is similar to the expression given in ref. [7].

The dynamic yield stress τ_s^{dyn} obtained with Casson's fits of experimental data are represented in Fig. 6 for cement (a.) and silica (b.) suspensions. It can be observed that it varies as a power function of the solid volume fraction ϕ as predicted by Eq. (8). The value found for the inverse of the exponent is $x \approx 0.12$ and $x \approx 0.11$ for cement and silica suspensions, respectively; x is slightly higher than the values found above. However the conclusions drawn above concerning the high compactness of the aggregates remain. The prefix constant obtained with the fit of τ_s^{dyn} leads to a range of 0.01–0.1 nN for the adhesion force F_a.

The static yield stress has also been reported in Fig. 6. It also varies as a power law of the solid volume fraction ϕ. However, since the aggregate size is determined from the balance between aggregate cohesion and flow related stresses, in the range 1 s^{-1} to 2000 s^{-1}, the model cannot be applied to static conditions.

4. Conclusion

The observed shear-thinning behaviour when decreasing shear stress steps are applied to cement or silica suspensions can be modelled by supposing the formation of aggregates. Here we follow the approach proposed by Mills and co-authors and introduce in the material law an effective volume fraction ϕ_{eff}, the aggregate volume fraction, that is a more relevant parameter in aggregated suspensions than the solid volume fraction ϕ. ϕ_{eff} is linked by a power law to the aggregate size, which can be expressed as a function of the adhesion force F_a and the shear stress τ. The determination of the power index and F_a allows one to predict the rheological behaviour of cement or silica suspensions of any solid volume fraction. The modelled curves obtained are in good agreement with experimental data. It has to be noticed that cement suspensions have a behaviour very similar to unreactive silica suspensions. In both cases, the aggregates formed are very compact. The origin of this high compactness may be the large solid concentrations of the studied suspensions (0.39 to 0.51).

The range of adhesion forces obtained seems to show that there are small interaction surfaces between particles, if the values of adhesion forces determined by AFM for calcium silicate hydrates C–S–H are supposed to be relevant here. This hypothesis is justified here because the nature of the interactions between unhydrated particles is presumed to be the same as the one between C–S–H at nano- and mesoscale. Due to the high values of pH and Ca^{2+} concentration, the cohesion forces are expected to be due to ionic correlations. The small values of interaction surfaces would then be linked to the fact that cement suspensions are observed during the dormant period, when the particles are only contacting at points.

References

[1] H. Van Damme, Et si le chatelier s'etait trompe? Ann. Ponts Chaussees 71 (1994) 30–41.
[2] B. Jönsson, H. Wennerström, A. Nonat, B. Cabane, Onset of cohesion in cement pastes, Langmuir 20 (2004) 6702–6709.
[3] R. Shaughnessy, P.E. Clark, The rheological behavior of fresh cement pastes, Cem. Concr. Res. 18 (1988) 327–341.
[4] D. Lootens. Ciment et suspensions concentrées modèles. Ecoulement, encombrement et floculation. PhD thesis, Université Paris 6, 2004.
[5] P. Mills, Non-Newtonian behaviour of flocculated suspensions, J. Physique, Lett. France 46 (1985) L301–L309.
[6] P. Mills, P. Snabre, The fractal concept in the rheology of concentrated suspensions, Rheol. Acta 26 (1988) 105–108.
[7] P. Snabre, P. Mills, Rheology of weakly flocculated suspensions of rigid particles, J. Phys. III France 6 (1996) 1811–1834.
[8] R.C. Sonntag, W.B. Russel, Structure and breakup of flocs subjected to fluid stresses, J. Colloid Interface Sci. 115 (1987) 378–389.
[9] P.D. Patel, W.B. Russel, A mean field theory for the rheology of phase separated or flocculated dispersions, Colloids Surf. 31 (1988) 355–383.
[10] A.A. Potanin, On the mechanism of aggregation in the shear flow of suspensions, J. Colloid Interface Sci. 145 (1991) 140–157.
[11] R. Wessel, R.C. Ball, Fractal aggregates and gels in shear flow, Phys. Rev., A 46 (1992) R3008–R3011.
[12] A.A. Potanin, R. De Rooij, D. Van der Ende, J. Mellema, Microrheological modeling of weakly aggregated dispersions, J. Chem. Phys. 102 (1995) 5845–5853.
[13] P. Snabre, L. Haider, M. Boynard, Ultrasound and light scattering from a suspension of reversible fractal clusters in shear flow, Eur. Phys. J., E 1 (2000) 41–53.
[14] R. Camargo, T. Palermo, Rheological properties of hydrate suspensions in an asphaltenic crude oil, Proc. of the 4th Int. Conf. on Gas Hydrates, Yokohama, Japan, 2002, pp. 880–885.
[15] A. Benhassaine, J.-C. Bénézet, Influence de la taille des particules sur la réactivité pouzzolanique des poudres de quartz, BLPC 1999/219, 1999.
[16] A. Benhassaine, J.-C. Bénézet, Contribution of the grain-size distribution of powder contents during the pozzolanic reaction within a lime phase, BLPC 2002/235, 2002.
[17] Q.D. Nguyen, H.A. Barnes, Rotating vane rheometry — a review, J. Non-Newton. Fluid Mech. 98 (2001) 1–14.
[18] N. Casson, A flow equation for pigment–oil suspensions of the printing ink type, in: C.C. Mill (Ed.), Rheology of Disperse Systems, Pergamon Press, London, 1959.
[19] L. Gmachowski, Estimation of the dynamic size of fractal aggregates, Colloids Surf., A 170 (2000) 209–216.
[20] K. Muhle, Floc stability in laminar and turbulent flow, in: B. Dobias (Ed.), Coagulation and Flocculation: Theory and Applications, Surfactant Science Series, vol. 47, 1993.
[21] A.A. Potanin, On the computer simulation of the deformation and breakup of colloidal aggregates in shear flow, J. Colloid Interface Sci. 157 (1993) 99–410.
[22] C. Selomulya, R. Amal, G. Bushell, T.D. Waite, Evidence of shear rate dependence on restructuring and breakup of latex aggregates, J. Colloid Interface Sci. 236 (2001) 67–77.
[23] C. Selomulya, G. Bushell, R. Amal, T.D. Waite, Understanding the role of restructuring in flocculation: the application of a population balance model, Chem. Eng. Sci. 58 (2003) 327–338.
[24] K.A. Kusters, J.G. Wijers, D. Thoenes, Aggregation kinetics of small particles in agitated vessels, Chem. Eng. Sci. 52 (1997) 107–121.
[25] C. Plassard, E. Lesniewska, I. Pochard, A. Nonat, Nanoscale experimental investigation of particle interaction at the origin of the cohesion of cement, Langmuir 21 (2005) 7263–7270.
[26] L. Nachbaur, J.C. Mutin, A. Nonat, L. Choplin, Dynamic mode rheology of cement and tricalcium silicate pastes from mixing to setting, Cem. Concr. Res. 31 (2001) 183–192.
[27] R.J.-M. Pellenq, N. Lequeux, H. Van Damme, Engineering the bonding scheme in C–S–H: the iono-covalent framework, Cem. Concr. Res. 38 (2008) 159–174.
[28] E.J. Windhab, Fluid immobilization — structure-related key mechanism for the viscous flow behavior of concentrated suspension systems, Appl. Rheol. 10 (2000) 134–144.